Supplemental material

The different mechanisms of GIP and GLP-1 action explain their different therapeutic efficacy in diabetes

E. Grespan, T. Giorgino, A. Natali, E. Ferrannini and A. Mari

1 Model and simulation details

The model used to study the effects of GIP and GLP-1 is an expansion of the model previously developed to describe the response to intravenous glucose [11].

1.1 Model equations

1.1.1 Immediately releasable pool dynamics equations

The core of the model, represented in Figure 1B of the main text, is the immediately releasable pool (IRP), which accounts for the insulin granules that undergo rapid exocytosis when intracellular calcium increases (triggering pathway). Over a longer time, insulin secretion is sustained by refilling of the IRP (amplifying pathway). Refilling is controlled by both calcium and glucose (through the refilling function). Calcium concentration is an input to the model and, along with glucose, is required to calculate insulin secretion. IRP dynamics are represented by the equation:

$$\frac{dQ}{dt} = -k(t)Q(t) + r(t) \tag{S.1}$$

where $Q(t)$ is the insulin mass in the IRP (measurements units depend on the experimental data, e.g., pmol per m^2 of estimated surface area), $k(t)$ is the calcium-controlled exocytosis rate constant (min^{-1}) and $r(t)$ is the refilling rate, dependent on both calcium and glucose (units are also experiment-specific, e.g., pmol min^{-1} m^{-2}).
The equations for k(t) and r(t) are:

$$k(t) = \partial_k\{f_k(C(t))\} \tag{S.2}$$

$$r(t) = \partial_r\{f_r(C(t), G(t))\} \tag{S.3}$$

To describe the dependence of $k(t)$ and $r(t)$ on calcium ($C(t)$, nmol/L) and glucose ($G(t)$, mmol/L), we use two functions, respectively $f_k(C(t))$ and $f_r(C(t), G(t))$, that are described in Section 1.1.2. The model assumes that a delay occurs between a change in glucose and calcium concentrations and the corresponding changes in $k(t)$ and $r(t)$. The delay is a combination of a time-shift and a first-order delay, and is represented in compact form with the operator $\partial\{\cdot\}$, where the subscript of $\partial\{\cdot\}$ indicates whether the delay refers to exocytosis or refilling. The delay functions are described in Section 1.1.3.
The instantaneous insulin secretion rate $S(t)$ (units are experiment-dependent, e.g., pmol $min^{-1}m^{-2}$) is:

$$S(t) = k(t)Q(t) \tag{S.4}$$

Equations (S.1)-(S.4), with initial steady-state conditions, provide the complete description of the model; insulin secretion can be predicted when both glucose and calcium are known.

1.1.2 Exocytosis and refilling functions

Both the exocytosis and the refilling functions $f_k(C)$ and $f_r(C,G)$ are based on the function of Mari et al. [12]:

$$\begin{aligned} &h(C;\rho,\gamma,\sigma_1,\sigma_2) = \\ &\sigma_1 C - \frac{1}{\tanh(\gamma\rho)+1}(\sigma_1-\sigma_2)\times \\ &\quad\times\left(C\tanh(\gamma\rho) - \frac{1}{\rho}\left(\log(\cosh(\gamma\rho)) - \log(\cosh(\rho(\gamma - C(t))))\right)\right) \end{aligned} \tag{S.5}$$

The function is represented in Figure S1. The parameter γ divides the C axis ($C \geq 0$) in two regions in which $h(C)$ is a quasi-linear function with low sensitivity σ_1 (left to γ) or high sensitivity σ_2 (right to γ). The parameter ρ influences the curvature around γ. The function was obtained analytically as the integral of the hyperbolic tangent function, shifted and scaled to satisfy the above requirements and, additionally, $h(0) = 0$ [12].

The exocytosis function is simply:

$$f_k(C;p_1,p_2,p_3,p_4) = h(C;p_1,p_2,p_3,p_4) \tag{S.6}$$

The parameters ρ, γ, σ_1 and σ_2 for $f_k(C)$ are thus p_1 to p_4. The refilling function is:

$$\begin{aligned} f_r(C,G;p_5,p_6,p_7,p_8,p_9,p_{10},p_{11}) = \\ p_5 + h\big(C;p_6,p_7,p_8 w(G,p_9,p_{10},p_{11}),w(G,p_9,p_{10},p_{11})\big) \end{aligned} \tag{S.7}$$

where

$$w(G;p_9,p_{10},p_{11}) = p_9 \frac{1}{2}\left[1+\tanh\left(p_{10}(G-p_{11})\right)\right] \tag{S.8}$$

In the refilling function, the sensitivities for C, σ_1 and σ_2, are modulated by glucose concentration G via the sigmoidal function $w(G)$. In addition, the ratio of the sensitivities is the constant $\sigma_1/\sigma_2 = p_8$ and $f_r(0,G) = p_5$.

1.1.3 Delay

The delay with which calcium and glucose exert their actions on exocytosis and refilling is a combination of a time shift τ and a first-order delay with time constant $1/\alpha$. This composite delay is indicated with the operator $\partial(\cdot)$; $y(t) = \partial(x(t))$ is obtained by the following delay differential equation:

$$\frac{dy(t)}{dt} = \alpha(x(t-\tau) - y(t)) \tag{S.9}$$

For exocytosis (∂_k), the parameters are $p_{12} = \tau$ and $p_{13} = \alpha$; for the refilling (∂_r), $p_{14} = \tau$ and $p_{15} = \alpha$.It should be noted that the delay has a different physiological interpretation for the calcium effect on $k(t)$ and for the refilling. For $k(t)$, the role of the time-shift is to accommodate for possibly imprecise alignment of the calcium and secretion data; the potential delayed effect of calcium on $k(t)$ is accounted by the first-order delay component. Thus, ∂_k has a minor role. For $r(t)$, the delay is an essential component of the description, as a delayed rise of the refilling is crucial to explain typical features of insulin secretion.

1.1.4 Glucose-induced potentiation

The delay of the refilling function described in Equation S.9 accounts for the gradual increase of insulin secretion after constant hyperglycemic stimulus. However, when the increase over time was not sufficient to reproduce a strong rising second-phase secretion elicited by hyperglycemic clamps, we introduced a time-dependent factor (K_{glu}) that multiplies the slope above the threshold of the refilling function f_r, *i.e.*, the last argument of the function h in Equation S.7. K_{glu} is 1 at baseline and progressively increases during the glucose stimulus to a value at the end of the experiment that depends on the specific study, which in our simulations ranges between 1.3 to 2.8. Results on the K_{glu} increase are reported in the supplementary figures below.

1.1.5 Glucose-calcium relationship

The calcium response to a glucose stimulus is obtained as a sum of a static function of glucose concentration, $C_s(G)$, and a dynamic component, $C_d(t)$ (Figure S2):

$$C(t) = C_s(G(t)) + C_d(t) \tag{S.10}$$

In the sigmoidal static function

$$C_s(G) = p_{16}\frac{1}{2}\left[1+\tanh\left(p_{17}(G-p_{18})\right)\right] \tag{S.11}$$

the parameters are derived from the glucose-calcium relationship reported in Henquin et al. [13].

The dynamic component $C_d(t)$ is obtained from a simple zero-gain linear system (with bi-dimensional state vector z) that generates a peak when glucose concentration is abruptly raised and a nonlinear function of glucose concentration that modulates the peak:

$$\frac{dz(t)}{dt} = \begin{bmatrix} -p_{19} & 0 \\ 0 & -p_{20} \end{bmatrix} z(t) + \begin{bmatrix} p_{19} \\ p_{20} \end{bmatrix} G(t) \qquad \text{with} \qquad z(0) = \begin{bmatrix} G(0) \\ G(0) \end{bmatrix} \tag{S.12}$$

$$C_d(t) = \max\left(0, \begin{bmatrix} 1 & -1 \end{bmatrix} z(t)\right) \left[\left(p_{21} - p_{22} \tanh(p_{23}(G(t) - p_{24})\right)\right] \tag{S.13}$$

1.1.6 Incretin effect on calcium

We assume that incretin hormones produce a transient increase in calcium. The peak increase varies in the different studies between 15 and 80 nmol/L and the duration of the peak varies between 15 and 30 minutes after the start of the incretin stimulus. In study B4, where a bolus of GIP was injected, the calcium peak is much higher (150 nmol/L in response to the low dose and 250 nmol/L in response to the high dose bolus) and it lasts 8 minutes. We assume that the effect of incretins is additive to that of glucose; therefore:

$$C_{total}(t) = C(t) + C_{incr}(t) \tag{S.14}$$

where $C(t)$ is the glucose-stimulated cytosolic calcium obtained from Equation S.10 and $C_{incr}(t)$ is the incretin-mediated transient increase in calcium. $C_{total}(t)$ is used in Equations S.5 - S.9 to reproduce the studies with incretin stimulation. $C_{incr}(t)$ was obtained in the various studies empirically, by fitting the model to the insulin secretion data. The mean $C_{incr}(t)$ in the various studies is reported in Table S3.

1.1.7 Incretin effect on refilling

We hypothesize that incretins increase the refilling function through a time-dependent factor K_{incr}; we assume that $K_{incr} = 1$ in the absence of incretin stimulation, while $K_{incr} > 1$ with incretin stimulation. The factor K_{incr} multiplies the slope above the threshold of the refilling function $f_r(C,G)$, i.e., the last argument of the function h in Equation S.7. When also glucose-induced potentiation (K_{glu}) is required, the slope above the threshold of the refilling function is multiplied by both K_{incr} and K_{glu}.

1.1.8 Calculation of the incretin effect on refilling from incretin hormones concentrations

The analysis of the mean K_{incr} values empirically calculated in the various studies versus the mean GIP or GLP-1 concentrations allowed us to define K_{incr}-hormone concentration relationships for GIP and GLP-1 (reported in Figure 5 of the main text). The equation describing the relationship between total GLP-1 concentration and the corresponding K_{incr} is:

$$K_{incrGLP1}(x) = \begin{cases} 1, & \text{if } x \leq \lambda_0. \\ 1 + \lambda(x - \lambda_0), & \text{if } x > \lambda_0. \end{cases} \tag{S.15}$$

where x is the measured GLP-1 concentration, λ_0 is a GLP-1 concentration threshold, below which it is assumed that GLP-1 does not affect the secretory response. In the curves reported in Figure 5 of the main text (light green lines), λ_0 was calculated as the mean value of the basal GLP-1 concentration of all studies; λ is the slope of the curve above λ_0 and was calculated empirically to fit the experimental data.
The relationship between total GIP concentration and the corresponding K_{incr} is given by the function:

$$K_{incrGIP}(x) = \begin{cases} 1, & \text{if } x \leq \eta_0. \\ 1 + \dfrac{K_{max}}{1 - \dfrac{1}{1 + exp(\theta\mu)}} \left(\dfrac{1}{1 + \exp(-\theta(x - \eta_0 - \mu))} - \dfrac{1}{1 + \exp(\theta\mu)} \right), & \text{if } x > \eta_0. \end{cases} \tag{S.16}$$

where x is the measured GIP concentration, $1+K_{max}$ is the function maximum value, θ determines the steepness of the curve transition from 1 to $1+K_{max}$, and μ influences the x-value at which the function value is $1+K_{max}/2$. η_0 is a GIP concentration threshold, below which it is assumed that GIP does not affect the secretory response. In the curves reported in Figure 5 of the main text (dark green lines) η_0 was calculated as the mean value of the basal GIP concentration of all studies. θ was calculated empirically to fit the data. The study of Nauck et al. [9] reported in Figure 6 of the main text and in Figure S10 is based on the relationships described by Equations S.15 and S.16.
In the OGTT and in the test with simultaneous infusion of GIP and GLP-1, the effects of GIP and GLP-1 were assumed to be additive and the total K_{incr} was calculated by the equation:

$$K_{incr}(x) = K_{incrGLP1}(x) + K_{incrGIP}(x) - 1 \tag{S.17}$$

The parameters used to calculate $K_{incrGIP}(x)$ and $K_{incrGLP1}(x)$ in Figure 5 of the main text and in Figure S10B are reported in Table S2.

1.2 Model code

An implementation of the model in the Matlab and Simulink languages is provided at the address `https://github.com/CNR-IN-MatMod/BetaCell2019`.

2 Supplementary tables

				NGT[a]								T2D[b]							
Par.	**Eq.**	**Description**	**Unit**	**Study A1**	**Study B1**	**Study B2**	**Study B3**	**Study B4**	**Study B5**	**Study C1**	**Study D1**	**Study A2**	**Study B1**	**Study B2**	**Study B3**	**Study B4**	**Study B5**	**Study C1**	**Study D2**
p1		ρ for exocytosis	$(nmol/L)^{-1}$	1.5	1.5	1.5	1.5	1.5	1.5	1.5	1.5	1.5	1.5	1.5	1.5	1.5	1.5	1.5	1.5
p2		γ for exocytosis	nmol/L	95	95	95	98	105	96.9	95	105	95	95	95	98	105	96.9	95	105
p3	S.1	σ_1 for exocytosis	$(nmol/L)^{-1}\times min^{-1}$	2.00×10^{-4}	2.00×10^{-4}	2.00×10^{-4}	2.00×10^{-4}	2.00×10^{-4}	2.00×10^{-4}	2.00×10^{-4}	2.00×10^{-4}	2.00×10^{-4}	2.00×10^{-4}	2.00×10^{-4}	2.00×10^{-4}	2.00×10^{-4}	2.00×10^{-4}	2.00×10^{-4}	2.00×10^{-4}
p4		σ_2 for exocytosis	$(nmol/L)^{-1}\times min^{-1}$	2.90×10^{-3}	2.90×10^{-3}	2.90×10^{-3}	2.90×10^{-3}	2.90×10^{-3}	2.90×10^{-3}	2.90×10^{-3}	2.90×10^{-3}	2.90×10^{-3}	2.90×10^{-3}	2.90×10^{-3}	2.90×10^{-3}	2.90×10^{-3}	2.90×10^{-3}	2.90×10^{-3}	2.90×10^{-3}
p5		$f_\tau(0, G)$	[S]	134	241	144	288	104.5	113.46	134	108	34.8	117.9	174	213	6.7	73.75	134	155.25
p6		ρ for refilling	$(nmol/L)^{-1}$	1.5	1.5	1.5	1.5	1.5	1.5	1.5	1.5	1.5	1.5	1.5	1.5	1.5	1.5	1.5	1.5
p7		γ for refilling	nmol/L	102	102	102	109	102	102	102	102	90	102	102	109	102	102	102	102
p8	S.3	σ_1/σ_2 for refilling	--	0	0	0	0	0	0	0	0	0	0	0	0	0	0	0	0
p9	S.4	σ_2 for refilling at $G\to\infty$	$[S]\times(nmol/L)^{-1}$	17.83	10.16	11.23	10.51	16.94	9.81	11.73	8.66	5.26	9.54	2.66	4.2	6.24	4.26	3.56	4.91
p10		w slope at G = p11	$(mmol/L)^{-1}$	0.0669	0.0669	0.0555	0.1302	0.0669	0.0555	0.0669	0.052	0.0669	0.0669	0.0555	0.1302	0.0669	0.0555	0.0669	0.052
p11		w glucose offset	mmol/L	13.18	13.18	18.3	17.02	13.18	18.31	13.18	7.8	13.18	13.18	18.31	17.02	13.18	18.31	13.18	7.8
p12	S.5	τ for exocytosis	min	0	0	0	0	0	0	0	0	0	0	0	0	0	0	0	0
p13	∂_k	α for exocytosis	min^{-1}	2.1	2.1	2.1	2.04	2.1	2.1	2.1	2.1	2.1	2.1	2.1	2.04	2.1	2.1	2.1	2.1
p14	S.5	τ for refilling	min	4.28×10^{-5}	4.28×10^{-5}	4.28×10^{-5}	4.28×10^{-5}	4.28×10^{-5}	4.28×10^{-5}	4.28×10^{-5}	4.28×10^{-5}	4.28×10^{-5}	4.28×10^{-5}	4.28×10^{-5}	4.28×10^{-5}	4.28×10^{-5}	4.28×10^{-5}	4.28×10^{-5}	4.28×10^{-5}
p15	∂r	α for refilling	min^{-1}	0.095	0.095	0.095	0.312	0.266	0.0665	0.095	0.095	0.095	0.095	0.095	0.624	0.266	0.095	0.095	0.095
p16		Cs max	nmol/L	256	256	256	256	256	256	256	256	256	256	256	256	256	256	256	256
p17	S.7	Cs slope at G = p18	$(mmol/L)^{-1}$	0.148	0.148	0.148	0.148	0.148	0.148	0.148	0.148	0.148	0.148	0.148	0.148	0.148	0.148	0.148	0.148
p18		Cs glucose offset	mmol/L	6.8	6.8	6.8	6.8	6.8	6.8	6.8	6.8	6.8	6.8	6.8	6.8	6.8	6.8	6.8	6.8
p19		Cd peak shape	min^{-1}	2	2	2	2	2	2	2	2	2	2	2	2	2	2	2	2
p20		Cd peak shape	min^{-1}	1.5	1.5	1.5	1.5	1.5	1.5	1.5	1.5	1.5	1.5	1.5	1.5	1.5	1.5	1.5	1.5
p21	S.8	Cd peak amplitude	nmol/L	10	10	10	10	10	10	10	10	10	10	10	10	10	10	10	10
p22	S.9	Cd peak amplitude	nmol/L	0.5	0.5	0.5	0.5	0.5	0.5	0.5	0.5	0.5	0.5	0.5	0.5	0.5	0.5	0.5	0.5
p23		Cd slope at G = p24	$(mmol/L)^{-1}$	15	15	15	15	15	15	15	15	15	15	15	15	15	15	15	15
p24		Cd glucose offset	mmol/L	120	120	120	120	120	120	120	120	120	120	120	120	120	120	120	120
K_{glu}	-	Max K_{glu} value	-	-	1.5	2.8	2.8	1.2	1.4	-	-	2.2	1.1	1.4	1.4	-	1.2	-	-

[a] Normal glucose tolerance; [b] Type 2 diabetes.

Table S1: Model parameters. [S] indicates the unit of insulin secretion, which is experiment-dependent.

Parameters	Equations	Reference curves		Study D1	Study D2
		NGT[a]	T2D[b]	NGT	T2D
λ_0 (pmol/L)	S.11	16	16	11	16
λ (pmol/L) $^{-1}$		0.08	0.056	0.19	0.001
η_0 (pmol/L)	S.12	24	24	15.5	24
K_{max}		1.1	0.6	1.1	0
θ (pmol/L) $^{-1}$		0.06	0.06	0.06	0.06
μ (pmol/L)		25	25	25	25

[a] Normal glucose tolerance; [b] Type 2 diabetes.

Table S2: Parameters for the calculation of the hormone concentrations-K_{incr} relationships described in Equations S.15 – S.17.

	GIP			GLP-1		
Study	Dose	NGT[a]	T2D[b]	Dose	NGT	T2D
A1	2	23	-	0.75	25	-
A2	4	-	31	1.2	-	31
B1	0.8	31	22	0.4	37	37
	2.4	32	32	1.2	39	39
B2	1.5	46	46	0.5	46	46
B3	4	53	53	1	-	53
	16	-	53	-	-	-
B4	1	88	73	-	-	-
	4	173	100	-	-	-
B5	8	46	46	1	46	46
C1	-	-	-	0.5	10	8
	-	-	-	1	17	13
	-	-	-	2	23	19
D1	1	12	-	0.3	12	-
D2	4	-	49	0.6	-	97

[a] Normal glucose tolerance; [b] Type 2 diabetes.

Table S3: Mean (as AUC/time) transient calcium increase above the glucose-stimulated levels. GIP and GLP-1 doses are in pmol·kg^{-1}·min^{-1}. In Study B4, GIP infusions were accompanied by a priming dose of 20 or 80 pmol/kg. In Study A1, the calcium profile is univocally determined by the data and independent of K_{incr}. In Studies B1-B5 the calcium profile is defined by the data, once K_{incr} is fixed. In the other studies, the calcium increase due to incretins was less clearly determinable. In these studies, we simulated a calcium rise that reproduced the data appropriately and was consistent with the other studies. The estimated effect on transient calcium increase was similar for GIP and GLP-1 and was preserved in T2D compared to NGT.

3 Supplementary figures

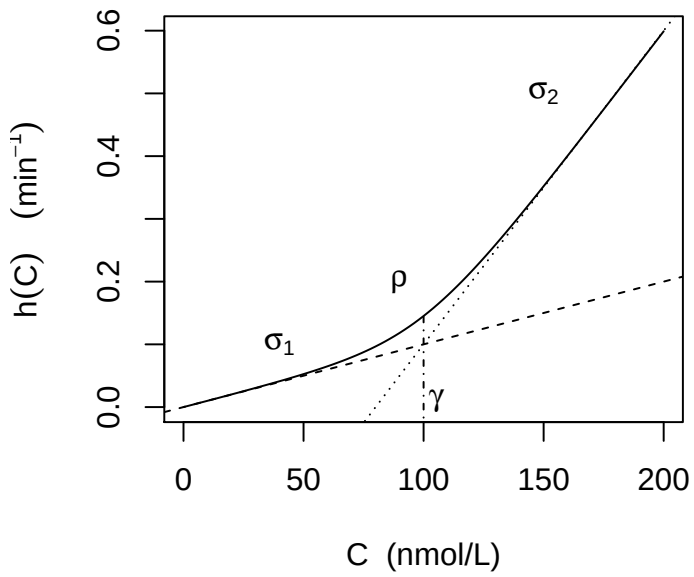

Figure S1: Function $h(C)$ used for exocytosis and refilling (Equation S.5). The scale of C, $h(C)$ and the parameters used in the plot are illustrative.

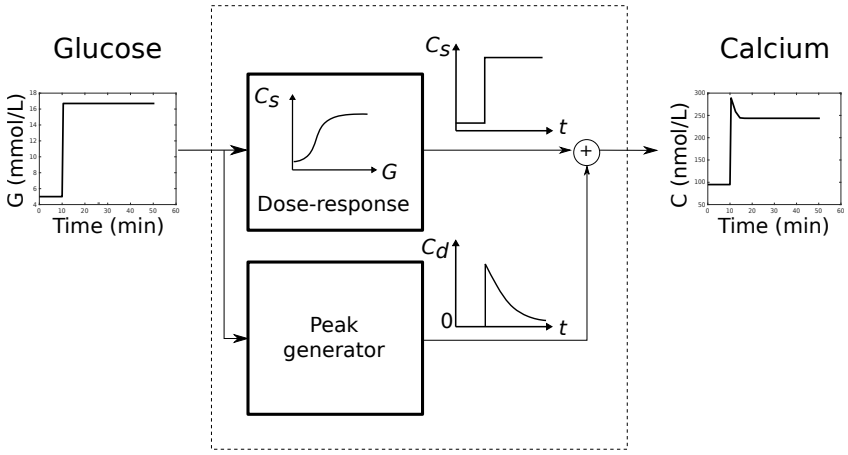

Figure S2: Scheme of the glucose-calcium model. The model predicts calcium from glucose based on the static dose-response (C_s, Equation S.11) and the addition of a calcium peak when glucose increases abruptly (C_d, Equations S.12- S.13).

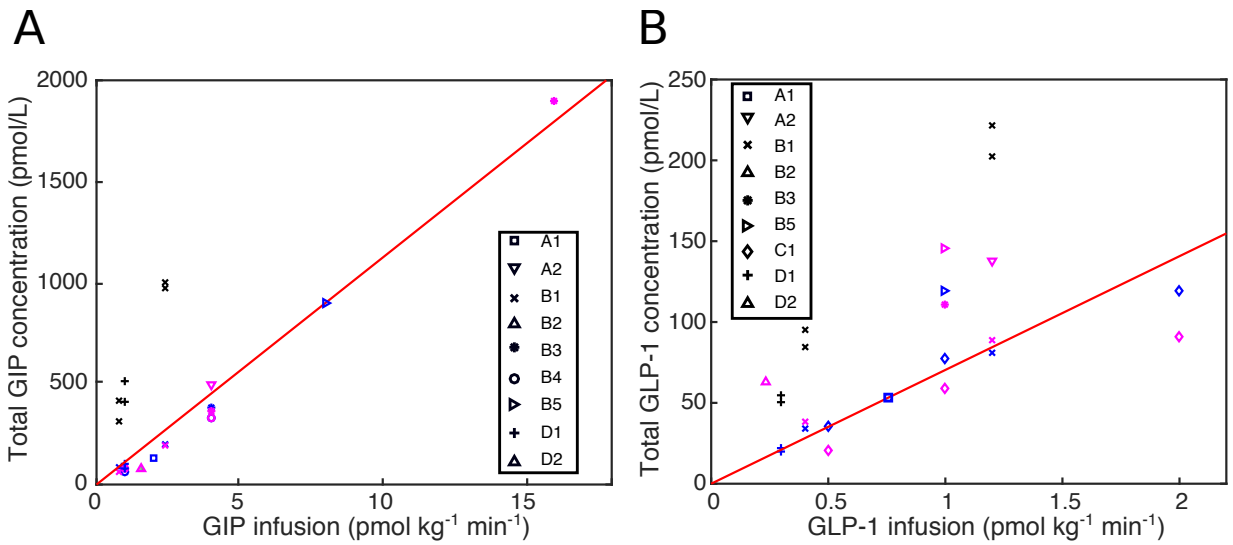

Figure S3: Relationships between GIP and GLP-1 infusion and average concentration in the studies considered in this work. As described in the Methods in the main text, the values in studies B1 and D1, which were obtained using an assay with very different characteristics, were rescaled. The black symbols show the values of the hormones concentrations before rescaling. The original values were 5 times greater for GIP and 2.5 times greater for GLP-1. In study B5, which reported only intact GIP, total GIP was extrapolated from the regression line (red line), given the dose. An analogous approach was used in study A1, in which only intact GLP-1 was available. The studies in NGT subjects are shown in blue and those in T2D subjects in purple.

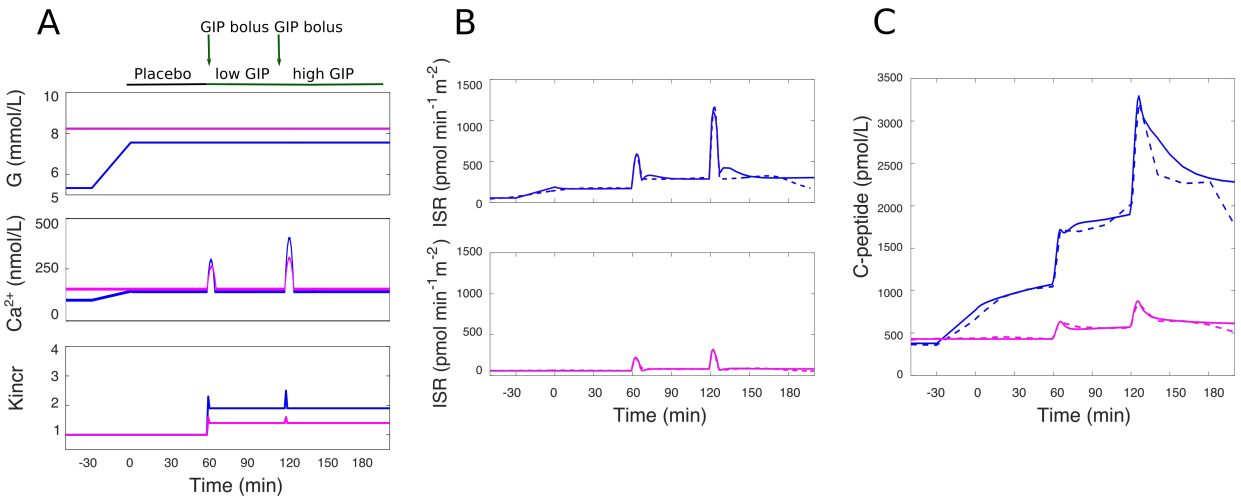

Figure S4: Simulation of Study B4, a hyperglycemic clamp with infusion of GIP at two doses in NGT (blue lines) and T2D (purple lines) subjects. A) Glucose (G) and Ca^{2+} concentrations and K_{incr}. With saline infusion, where $K_{incr} = 1$, the gradual increase with time in insulin secretion in NGT subjects is simulated by an increase in K_{glu}, which rises to 1.2 at the end of the test. The increase is absent in T2D subjects. B) Simulated (continuous lines) and C-peptide-derived insulin secretion (ISR) (dashed lines). C) Simulated (continuous lines) and measured C-peptide concentration (dashed lines). In correspondence to the GIP boluses, which cause a brisk peak in GIP concentration, both calcium and K_{incr} exhibit a spike, which contribute to the insulin secretion peak.

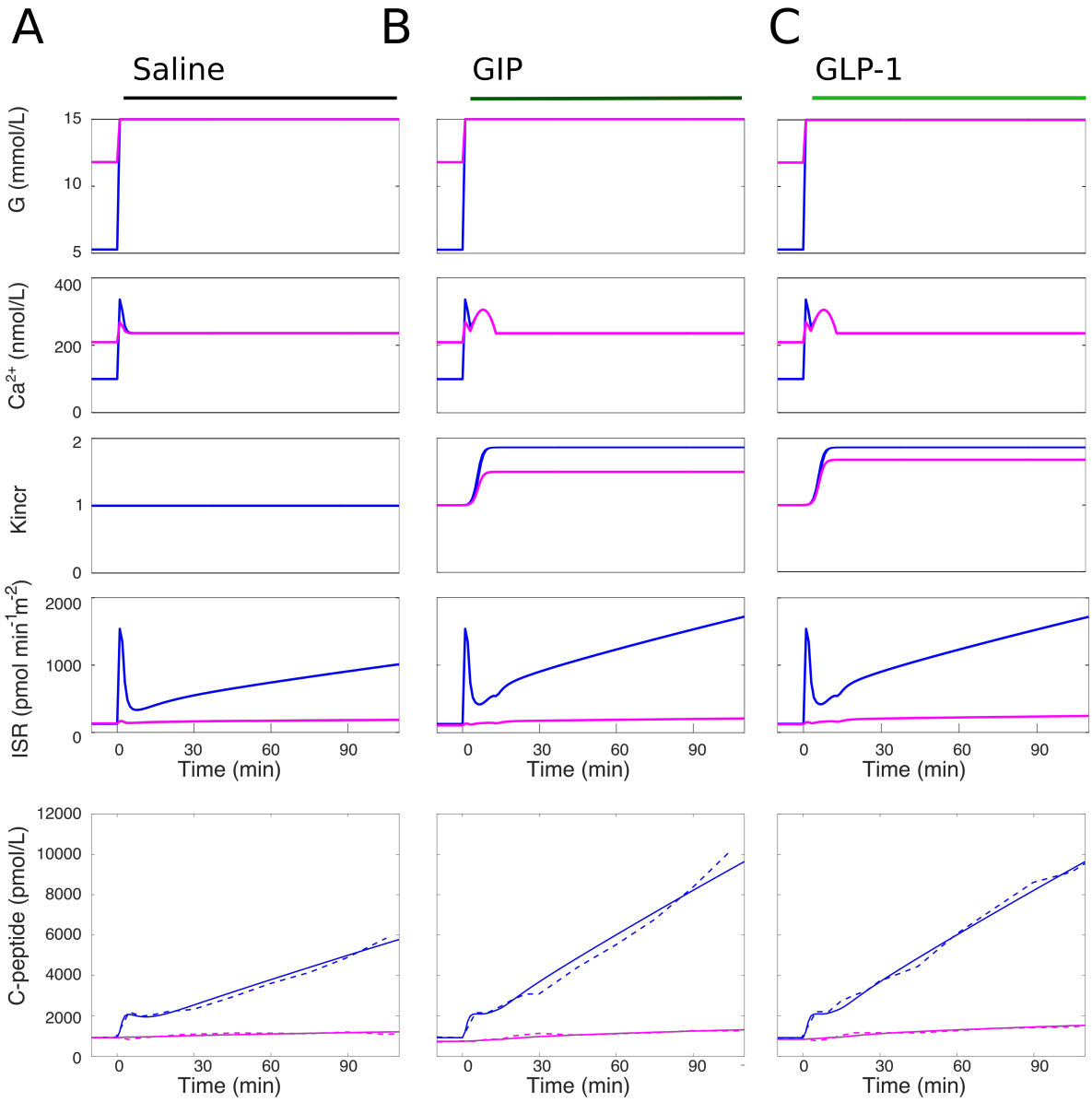

Figure S5: Simulation of Study B2, a hyperglycemic clamp with continuous infusion of saline (A), GIP (B) or GLP-1 (C) in NGT subjects (blue lines) or T2D subjects (purple lines). The panels show glucose (G) and Ca^{2+} concentrations, K_{incr}, insulin secretion (ISR) and simulated (continuous lines) and measured (dashed lines) C-peptide concentration. With saline infusion, where $K_{incr} = 1$, ramping insulin secretion is simulated by a gradual increase in K_{glu}, which rises to 2.8 at the end of the test in NGT subjects and to 1.4 in T2D subjects. It is hypothesized that the same K_{glu} increase underlies also the GIP and GLP-1 infusion tests, in which the greater increase in insulin secretion is explained by K_{incr}, determined empirically.

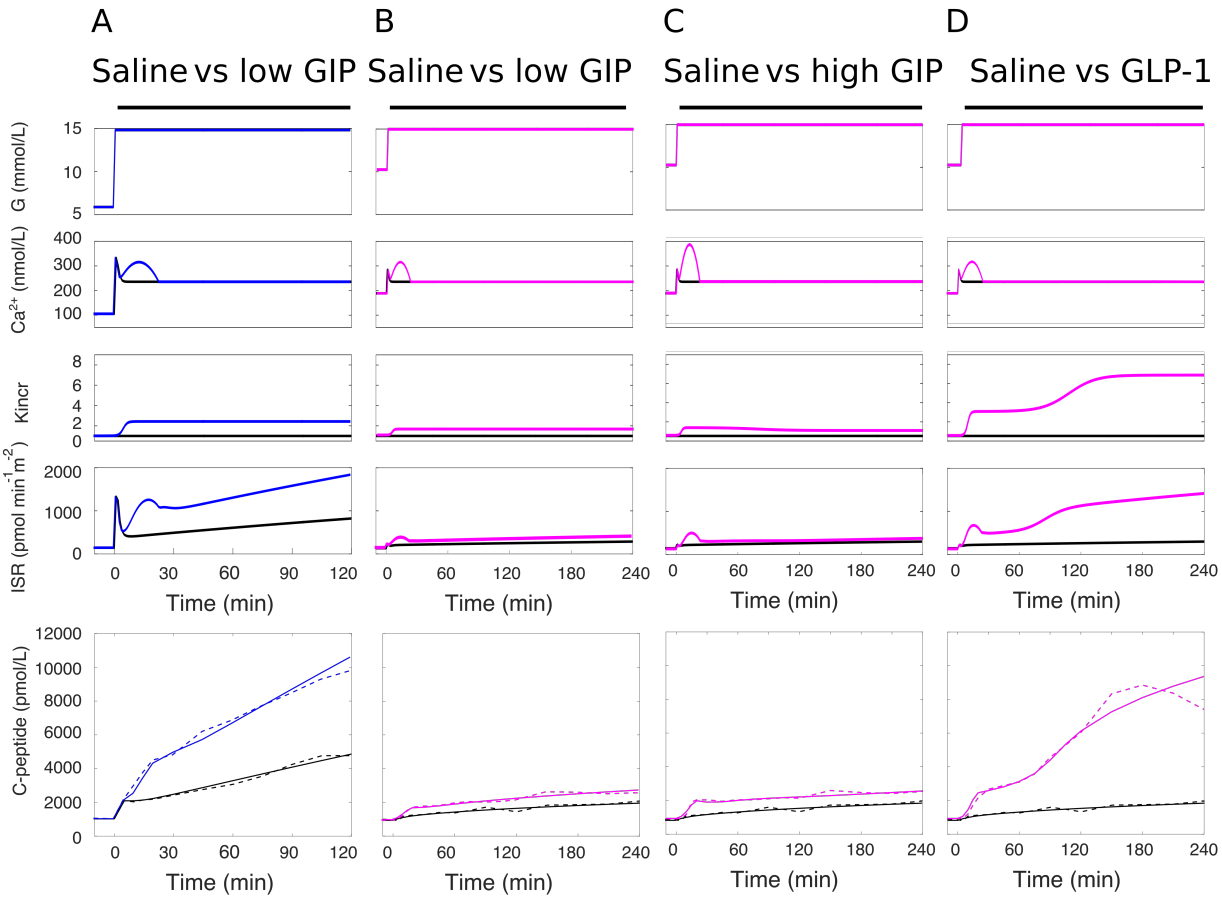

Figure S6: Simulation of Study B3, a hyperglycemic clamp with infusion of saline, GIP at low and high dose, and GLP-1, in NGT (blue lines, panel A) and T2D (purple lines, panels B-D) subjects. All panels show the saline (black lines) and incretin-stimulated (colored lines) results superimposed. The panels show glucose (G) and Ca^{2+} concentrations, K_{incr}, insulin secretion (ISR) and simulated (continuous lines) and measured (dashed lines) C-peptide concentration. With saline infusion, where $K_{incr} = 1$, ramping insulin secretion is simulated by a gradual increase in K_{glu}, which rises to 2.8 at the end of the test in NGT subjects and 1.4 in T2D subjects. It is hypothesized that the same K_{glu} increase underlies also the GIP and GLP-1 infusion tests, in which the greater increase in insulin secretion is explained by K_{incr}, determined empirically. K_{incr} in panels B and C is similar, despite the very different GIP doses (4 pmol·kg^{-1}·min^{-1}in panel B and 16 pmol·kg^{-1}·min^{-1} in panel C), indicating that the effect of GIP saturates. At the low GIP dose, K_{incr} in NGT subjects (panel A) was higher than in T2D subjects (panel B), but far lower than that reached during GLP-1 infusion in T2D subjects (panel D).

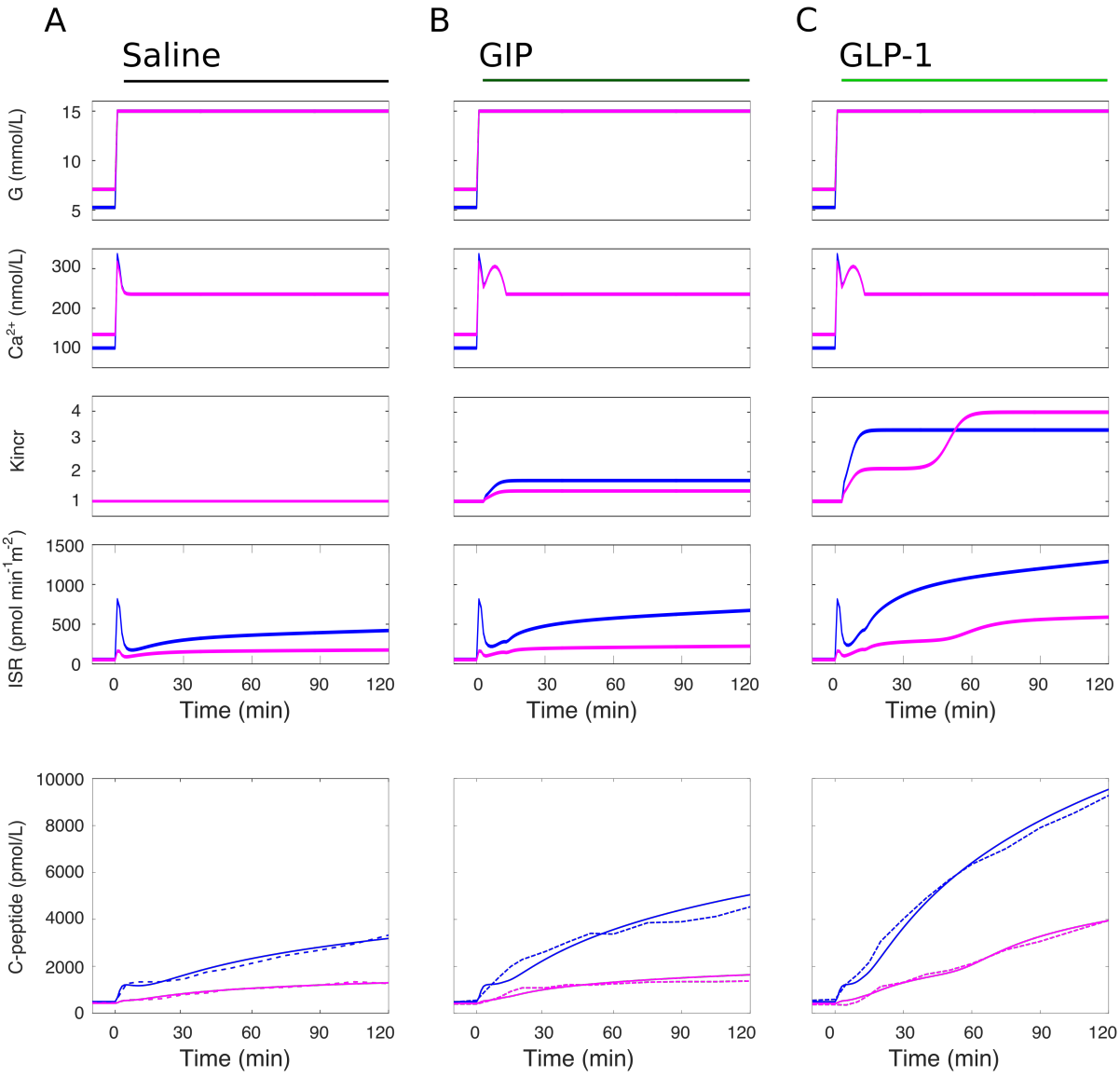

Figure S7: Simulation of Study B5, a hyperglycemic clamp with continuous infusion of saline (A), GIP (B) or GLP-1 (C) in NGT subjects (blue lines) or T2D subjects (purple lines) with chronic pancreatitis. The panels show glucose (G) and Ca^{2+} concentrations, K_{incr}, insulin secretion (ISR) and simulated (continuous lines) and measured (dashed lines) C-peptide concentration. With saline infusion, where $K_{incr} = 1$, ramping insulin secretion is simulated by a gradual increase in K_{glu}, which rises to 1.4 at the end of the test in NGT subjects and to 1.2 in T2D subjects. It is hypothesized that the same K_{glu} increase underlies also the GIP and GLP-1 infusion tests, in which the greater increase in insulin secretion is explained by K_{incr}, determined empirically

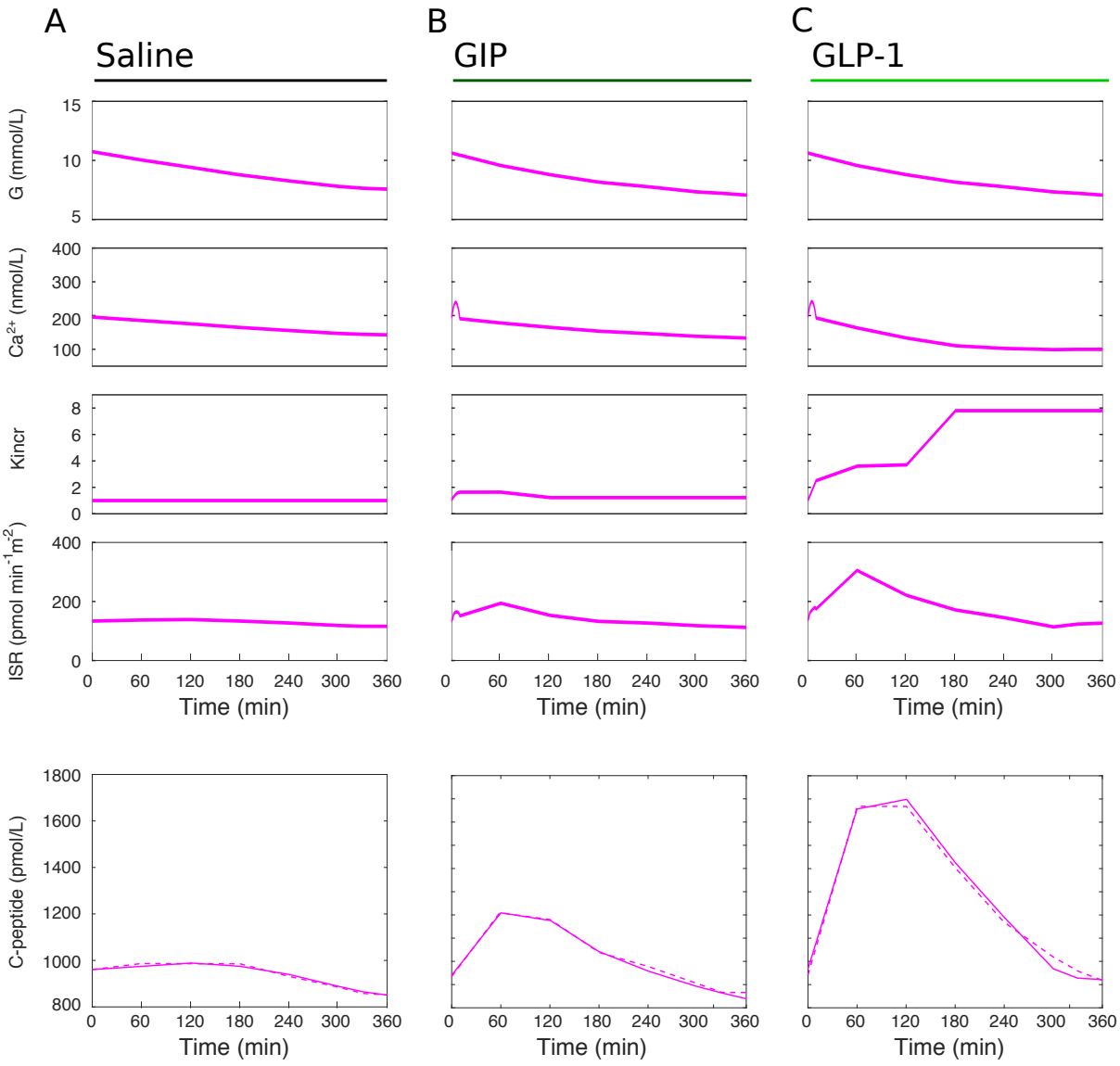

Figure S8: Simulation of Study A2, an infusion of saline (A), GIP (B) or GLP-1 (C) in T2D subjects, starting at basal glucose. With saline infusion, where $K_{incr} = 1$, the fall in insulin secretion with falling glucose is prevented by an increase in K_{glu}, which rises to 2.2 at the end of the test. It is hypothesized that the same K_{glu} increase underlies also the GIP and GLP-1 infusion tests, in which the greater increase in insulin secretion is explained by K_{incr}, determined empirically. With GIP infusion, the increase in K_{incr} is modest (1.3 on average) in spite of the high hormone levels, while with GLP-1 it is much greater (5.9 on average).

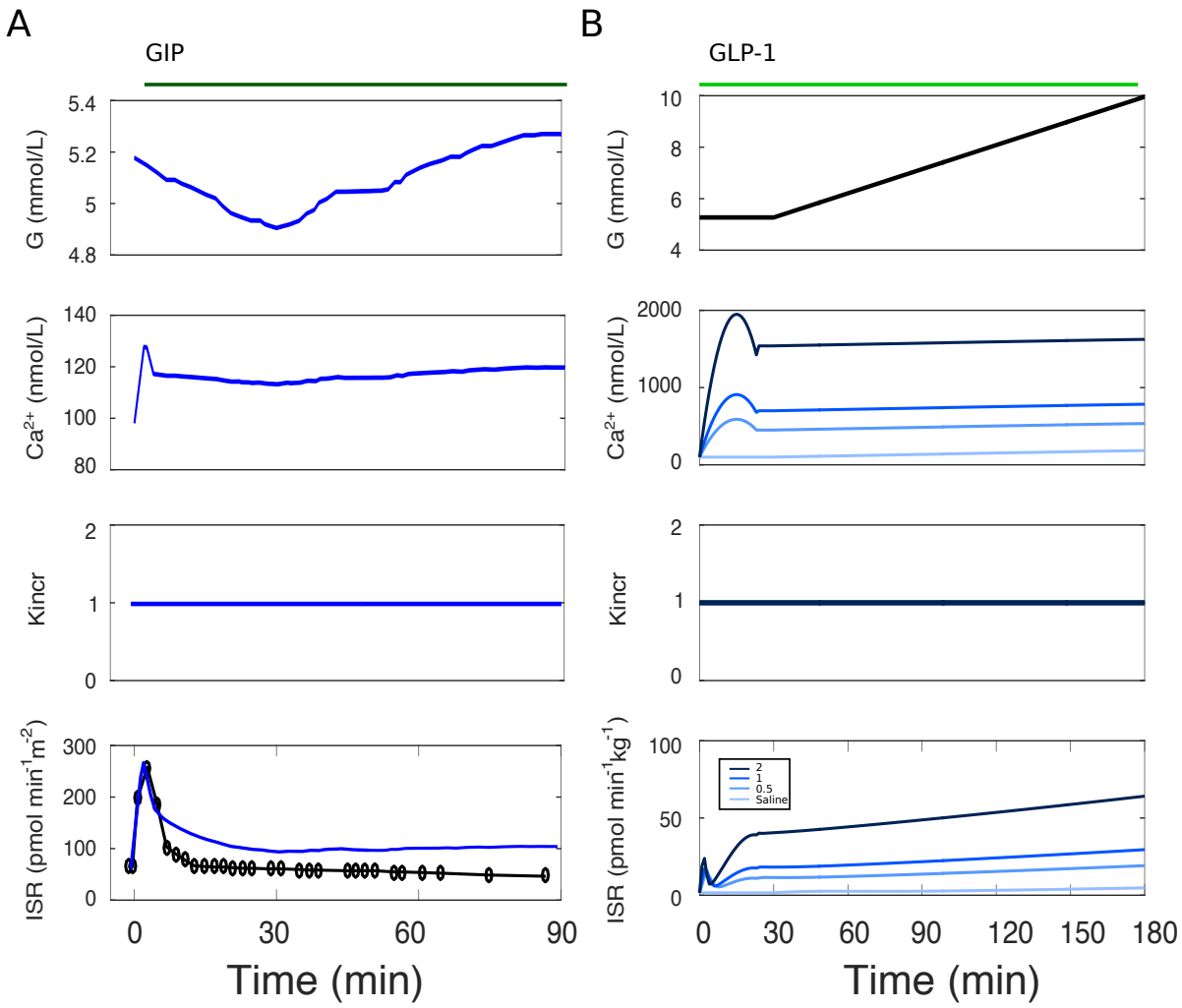

Figure S9: Simulation of the effects of sustained elevated calcium as a possible action of incretin hormones. The panels show glucose (G) and Ca^{2+} concentrations, K_{incr} and insulin secretion (ISR). In all simulations $K_{incr} = 1$. A) Protracted, rather than transient, calcium elevation in Study A1 (to $\sim$120 $nmol/L$ from a baseline of $\sim$100 $nmol/L$) would produce a sustained increase in insulin secretion, in disagreement with the data (black line in the lowest panel). B) In the graded glucose infusion study with GLP-1 infusion (Study C1), the observed strong increase in insulin secretion with high GLP-1 doses could be explained by an effect on calcium alone. However, this hypothesis would require highly supraphysiological calcium levels.

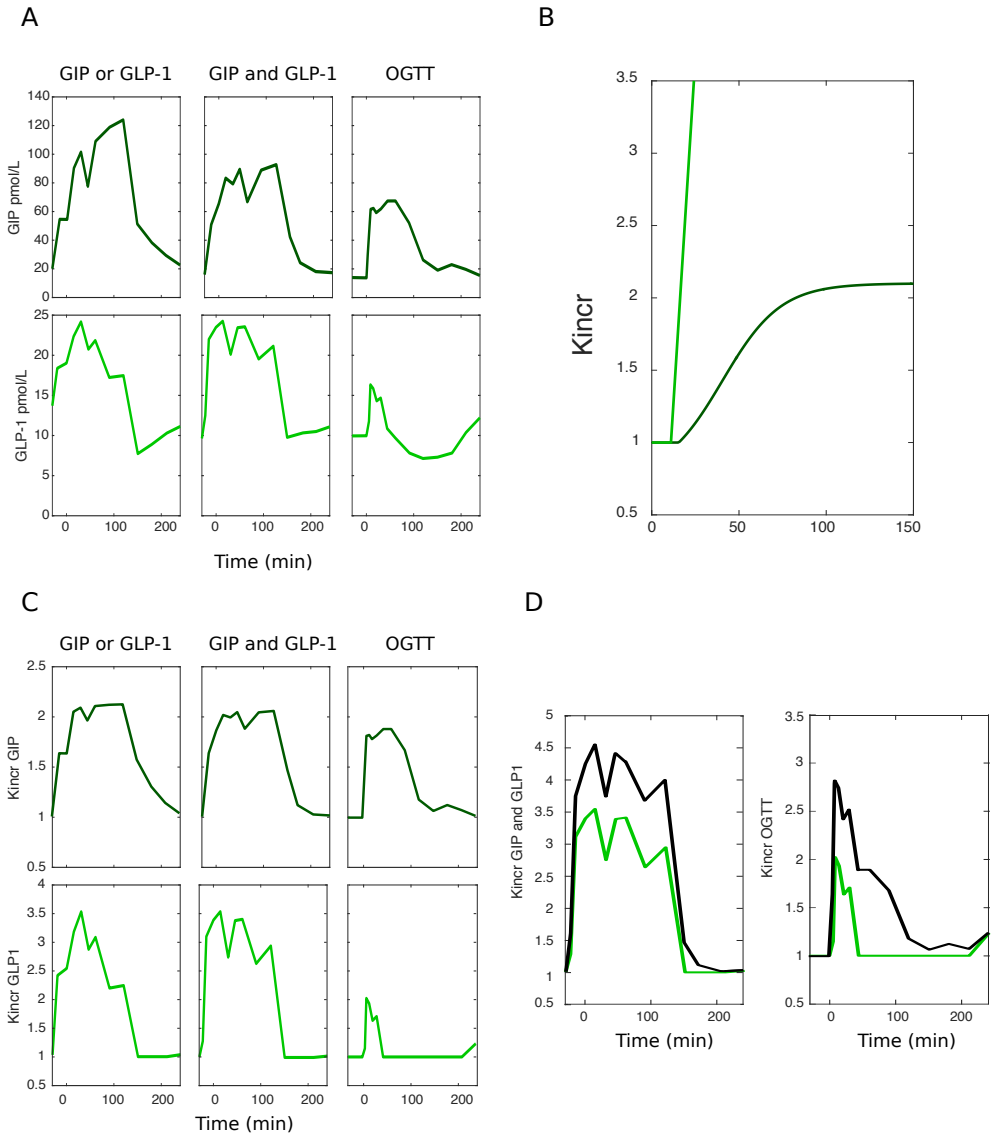

Figure S10: Calculation of K_{incr} from GIP and GLP-1 measured concentrations in the tests of Study D1, reported in Figure 6 of the main text. A) Total GIP (dark green) and GLP-1 (light green) concentrations measured in the tests with separate GIP or GLP-1 infusions (left), GIP and GLP-1 co-infusion (middle) and OGTT (right). B) Relationships between K_{incr} and GIP (Equation S.16, dark green) and GLP-1 (Equation S.15, light green) concentrations for this study, adapted from Figure 5 of the main text. C) K_{incr} calculated from GIP and GLP-1 concentrations of panel A, using the relationships of panel B. The K_{incr} values of the left panel column were used in the simulations reported in Figures 6B an 6C of the main text. D) K_{incr} calculated in the test with GIP and GLP-1 co-infusion (left panel, black line) and in the OGTT (right panel, black line), assuming an additive effect (Equation S.17). The green lines in both panels represent the contribution to K_{incr} due to GLP-1. The difference between the black and the green lines represent the contribution to K_{incr} due to GIP. The K_{incr} values plotted in black were used in the simulation reported in Figures 6D and 6E of the main text.

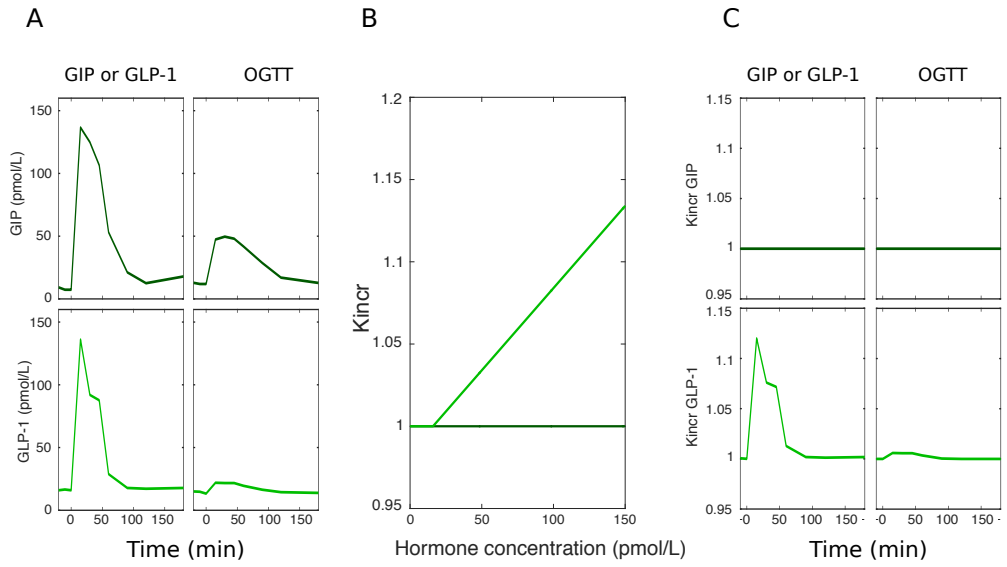

Figure S11: Calculation of K_{incr} from GIP and GLP-1 measured concentrations in Study D2, reported in Figure 7 of the main text. A) Total GIP (dark green) and GLP-1 (light green) concentrations measured in the tests with separate GIP or GLP-1 infusion (left), and OGTT (right). B) Relationships between K_{incr} and GIP (Equation S.16, dark green) and GLP-1 (Equation S.15, light green) concentrations for this study. C) K_{incr} calculated from GIP and GLP-1 concentrations of panel A, using the relationships of panel B. These K_{incr} values were used in the simulations reported in Figures 7B (GIP infusion), 7C (GLP-1 infusion) and 7D (OGTT) of the main text.

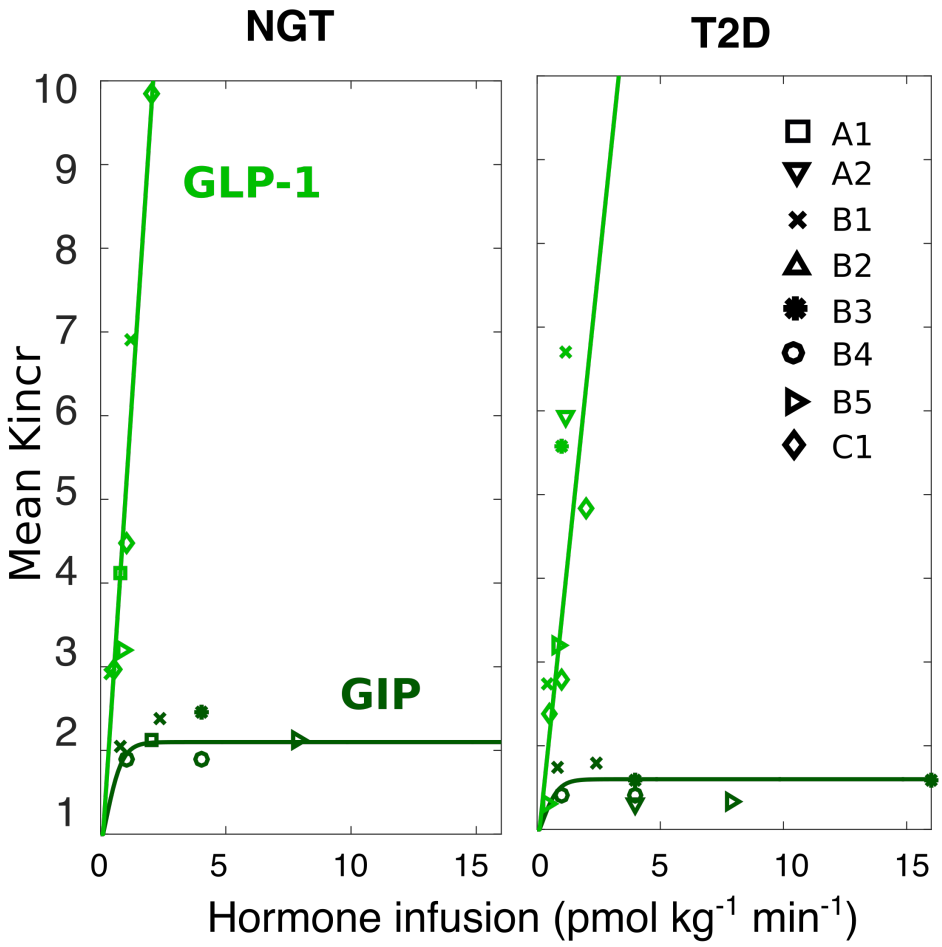

Figure S12: Relationships between K_{incr} and GIP (dark green lines) or GLP-1 (light green lines) infusion in the studies with incretin hormone infusion, represented by the different markers. This figure reproduces the results of Figure 5 of the main text, using in the abscissa the hormone infusion instead of the concentration.

4 References

[1] Honka H, Koffert J, Kauhanen S, Kudomi N, Hurme S, Mari A, et al. Liver blood dynamics after bariatric surgery: the effects of mixed-meal test and incretin infusions. Endocr Connect. 2018;7:888–896.

[2] Mentis N, Vardarli I, Köthe LD, Holst JJ, Deacon CF, Theodorakis M, et al. GIP Does Not Potentiate the Antidiabetic Effects of GLP-1 in Hyperglycemic Patients With Type 2 Diabetes. Diabetes. 2011;60:1270–1276.

[3] Nauck MA, Heimesaat MM, Ørskov C, Holst JJ, Ebert R, Creutzfeldt W. Preserved incretin activity of glucagon-like peptide 1 [7-36 amide] but not of synthetic human gastric inhibitory polypeptide in patients with type-2 diabetes mellitus. J Clin Invest. 1993;91:301–307.

[4] Højberg PV, Vilsbøll T, Raøl R, Knop FK, Bache M, Krarup T, et al. Four weeks of near-normalisation of blood glucose improves the insulin response to glucagon-like peptide-1 and glucose-dependent insulinotropic polypeptide in patients with type 2 diabetes. Diabetologia. 2009;52:199–207.

[5] Vilsbøll T, Krarup T, Madsbad S, Holst JJ. Defective amplification of the late phase insulin response to glucose by GIP in obese Type II diabetic patients. Diabetologia. 2002;45:1111–1119.

[6] Meier JJ, Gallwitz B, Kask B, Deacon CF, Holst JJ, Schmidt WE, et al. Stimulation of insulin secretion by intravenous bolus injection and continuous infusion of gastric inhibitory polypeptide in patients with type 2 diabetes and healthy control subjects. Diabetes. 2004;53:S220–S224.

[7] Knop FK, Vilsbll T, Hjberg PV, Larsen S, Madsbad S, Holst JJ, et al. The insulinotropic effect of GIP is impaired in patients with chronic pancreatitis and secondary diabetes mellitus as compared to patients with chronic pancreatitis and normal glucose tolerance. Reg Pept. 2007 Dec;144(1-3):123–130.

[8] Kjems LL, Holst JJ, Vlund A, Madsbad S. The influence of GLP-1 on glucose-stimulated insulin secretion. Diabetes. 2003;52:380–386.

[9] Nauck MA, Bartels E, Ørskov C, Ebert R, Creutzfeldt W. Additive insulinotropic effects of exogenous synthetic human gastric inhibitory polypeptide and glucagon-like peptide-1-(7-36) amide infused at near-physiological insulinotropic hormone and glucose concentrations. J Clin Endocrinol Metab. 1993;76:912–917.

[10] Lund A, Vilsbll T, Bagger JI, Holst JJ, Knop FK. The separate and combined impact of the intestinal hormones, GIP, GLP-1, and GLP-2, on glucagon secretion in type 2 diabetes. Am J Physiol Endocrinol Metab. 2011 Jun;300(6):E1038–E1046.

[11] Grespan E, Giorgino T, Arslanian S, Natali A, Ferrannini E, Mari A. Defective amplifying pathway of β-cell secretory response to glucose in type 2 diabetes: integrated modeling of in vitro and in vivo evidence. Diabetes. 2018;67(3):496–506.

[12] Mari A, Tura A, Gastaldelli A, Ferrannini E. Assessing insulin secretion by modeling in multiple-meal tests: role of potentiation. Diabetes. 2002;51(suppl 1):S221–226.

[13] Henquin JC, Nenquin M, Stiernet P, Ahren B. In vivo and in vitro glucose-induced biphasic insulin secretion in the mouse pattern and role of cytoplasmic Ca^{2+} and amplification signals in β-cells. Diabetes. 2006;55:441–451.